SLAC–PUB–7574
June 1997

PRELIMINARY MEASUREMENT OF PROMPT $D^{\pm}$ AND $D^{*\pm}$ MESON PRODUCTION AND $D^{*\pm}$ SPIN ALIGNMENT IN HADRONIC Z^0 DECAYS*

The SLD Collaboration**
Stanford Linear Accelerator Center
Stanford University, Stanford, CA 94309

ABSTRACT

We have measured the production rates as a function of scaled energy x of prompt charmed pseudoscalar $D^{\pm}$ and vector $D^{*\pm}$ mesons in hadronic Z^0 decays. The prompt signal components were isolated from the background of D mesons from B hadron decays using impact parameters of reconstructed $D^{\pm} \to K^{\mp}\pi^{\pm}\pi^{\pm}$ and D^*-daughter $D^0 \to K^-\pi^+$ and $D^0 \to K^-\pi^+\pi^-\pi^+$ candidates. Using the combined meson production rates we have measured the fraction of hadronic Z^0 decays into $c\bar{c}$, $R_c = 0.182 \pm 0.027$ (stat.) ± 0.012 (syst.) (Preliminary). Comparison of the $D^{*\pm}$ and $D^{\pm}$ rates gives a direct probe of vector (V) vs. pseudoscalar (P) meson production for charmed quarks, and for $x > 0.4$ we have measured $P_V = V/(V+P) = 0.65 \pm 0.09(stat.) \pm 0.03(syst.) \pm 0.03$ (BR) (Preliminary). We have measured the degree of spin alignment of the $D^{*\pm}$ mesons along their flight direction and find it to be consistent with zero. We compared the latter two results with QCD- and model-based predictions of charm-quark jet fragmentation.

Contributed to the XVIII International Symposium on Lepton Photon Interactions, July 28 - August 1 1997, Hamburg, Germany, and to the International Europhysics Conference on High Energy Physics, 19-26 August 1997, Jerusalem, Israel; Ref: 290.

1 Introduction

The fragmentation of heavy quarks has been studied both theoretically and experimentally. Some of the theoretical models are quite successful in describing experimental data collected in e^+e^- annihilation. In addition, the total production rate of charmed mesons can be used to derive the fraction of hadronic Z^0 decays into charm-anticharm pairs, $R_c = \Gamma_{Z^0\to c\bar{c}}/\Gamma_{Z^0\to hadrons}$. Spin-dependent properties of the fragmentation, such as the relative vector to pseudoscalar meson production ratio or the spin alignment of vector mesons, may be useful in studying the dynamics.

The quantity P_V, defined as the relative production ratio of vector (V) to (vector+pseudoscalar (P)) mesons, is expected in a naive spin-counting model to be $P_V = V/(V+P) = 0.75$ for promptly produced mesons. For charmed mesons produced in $Z^0 \to c\bar{c}$ events recent measurements from LEP have yielded values lower than this expectation, $P_V = 0.53 \pm 0.16$ [1] and 0.54 ± 0.10 [2]. Models for charm fragmentation based on perturbative QCD, by Suzuki [3] and by Braaten et al. [4], predict a dependence of P_V on the fractional energy carried by the meson, $x_D = 2E_D/\sqrt{s}$, where E_D is the energy of the charmed meson and $\sqrt{s}$ is the c.m. energy. The degree of vector meson spin alignment along the flight direction is expected to be zero in the naive spin-counting model; in the calculations of Suzuki and Braaten et al., this also depends on x_D [3, 4].

Here we present the preliminary results of a study of the production of prompt charged vector and pseudoscalar charmed mesons in Z^0 decay events produced by the SLAC Linear Collider (SLC) and recorded in the SLC Large Detector (SLD). Those mesons produced promptly were separated from those produced in decays of B-hadrons, as well as from combinatoric background, using lifetime information. The prompt component was then extracted independent of assumptions about D-meson production from B-hadron decays. From the number of prompt charged D^{*+} and D^+ mesons[*] we derived a measurement of R_c. Since neutral D^{*0} mesons cannot decay into charged D^+ mesons, this measures directly the number of primary charm quarks that pair with anti-d quarks, $N_{c\bar{d}}$, and the R_c value is relatively insensitive to assumptions about the other charmed hadrons produced. By comparing the number of D^{*+} and D^+ mesons found, we measured P_V as a function of x_D. This measurement is also

[*]The inclusion of charge-conjugate states is implied throughout this paper.

insensitive to D^{*0} production and decay. We also measured the degree of spin alignment of D^{*+} mesons along their flight direction as a function of x_D. We compare our results with those from other Z^0 and lower energy experiments, as well as with the predictions of the spin-counting model and the models of Suzuki and of Braaten et al.

2 Apparatus and Hadronic Event Selection

The e^+e^- annihilation events produced at the Z^0 resonance by the SLC have been recorded in the SLD, a general description of which can be found elsewhere [5]. Charged tracks are measured in the central drift chamber (CDC) [6] and in the vertex detector (VXD) [7]. Momentum measurement is provided by a uniform axial magnetic field of 0.6 T. The VXD is composed of CCDs containing a total of 120 million $22 \times 22 \mu\text{m}^2$ pixels arranged in four concentric layers of radius between 2.9 and 4.2 cm. Including the uncertainty on the primary interaction point (IP), the CDC and VXD give a combined impact parameter resolution in the (x-y) plane transverse to the beam axis of $11 \oplus 70/(p_\perp \sqrt{\sin\theta}) \mu$m, where $p_\perp$ is the track momentum transverse to the beam axis in GeV/c and θ is the track polar angle with respect to the beamline. Particle energies are measured in the Liquid Argon Calorimeter (LAC) [8], which contains both electromagnetic and hadronic sections, and in the Warm Iron Calorimeter [9].

Three triggers were used for hadronic events. The first required a total LAC electromagnetic energy greater than 12 GeV; the second required at least two well-separated tracks in the CDC; and the third required at least 4 GeV in the LAC and one track in the CDC.

This analysis used the charged tracks measured in the CDC and VXD. A set of cuts was applied to the data to select well-measured tracks and events well-contained within the detector acceptance. Charged tracks were required to have (i) a closest approach transverse to the beam axis within 5 cm, and within 10 cm along the axis from the measured interaction point; (ii) a polar angle θ with respect to the beam axis within $|\cos\theta| < 0.80$; and (iii) a momentum transverse to the beam axis, $p_\perp > 0.15$ GeV/c. Events were required to have (i) a minimum of five such tracks; (ii) a thrust axis [10] polar angle within $|\cos\theta_T| < 0.71$; and (iii) a total visible energy E_{vis} of at least 20 GeV, which was calculated from the selected tracks assigned the charged pion mass. From our 1993-95 data sample 102,564 events passed these cuts. The efficiency for selecting hadronic events satisfying the $|\cos\theta_T|$ cut was estimated to be above 96%. The background in the selected event sample was estimated to be $0.3 \pm 0.1\%$, dominated by $Z^0 \to \tau^+\tau^-$ events. Distributions of single particle and event topology observables in the selected events were found [11] to be well described by Monte Carlo models of hadronic Z^0 decays [12, 13] combined with a simulation of the SLD.

3 Initial Selection of D^{*+} and D^+ Candidates

Observed D^{*+} and D^+ mesons can be produced in $Z^0 \to c\bar{c}$ events, as well as from B hadron decays in $Z^0 \to b\bar{b}$ events. We describe the first category as primary mesons, and the second as secondary mesons. We first applied a set of cuts to select D mesons and reduce combinatoric background. We then divided the candidates as described in the next section into samples enriched in primary (c-rich) and secondary (b-rich) decays. From the measured numbers of observed charmed mesons in the two samples, we derived the primary and secondary production rates.

The D^{*+} mesons were identified using the decay $D^{*+} \to D^0\pi_s^+$ followed by $D^0 \to K^-\pi^+$ ($K\pi$ mode) or $D^0 \to K^-\pi^+\pi^-\pi^+$ ($K\pi\pi\pi$ mode). We first searched for D^0 candidates via the $K\pi$ and $K\pi\pi\pi$ decay modes. Each event was divided into two hemispheres by the plane perpendicular to the thrust axis. In each hemisphere we considered all two- ($K\pi$) or four- ($K\pi\pi\pi$) track combinations of net charge zero, and assigned the charged kaon mass in turn to one of the particles and the charged pion mass to the other(s). For the $K\pi\pi\pi$ mode all tracks were required to have $p > 0.75$ GeV/c. If the invariant mass of a D^0 candidate was in the range $1.765 < M_{K\pi} < 1.965$ GeV/c^2 ($K\pi$) or $1.795 < M_{K\pi\pi\pi} < 1.935$ GeV/c^2 ($K\pi\pi\pi$), it was combined with each π_s candidate track having charge opposite that of the K candidate to form a set of D^{*+} candidates.

We required D^{*+} candidates to pass one of two sets of cuts designed to reduce combinatoric background. The first set exploited the facts that D mesons are produced with relatively high momentum and decay isotropically; we required: (1.i) $x_{D^*} > 0.4$ ($K\pi$) or >0.5 ($K\pi\pi\pi$); (1.ii) $|\cos\theta_K^0| < 0.9$ ($K\pi$) or <0.8 ($K\pi\pi\pi$), where θ_K^0 is the angle between the direction of the D^0 candidate in the laboratory frame and the K

candidate in the D^0 rest frame; and (1.iii) $p_{\pi_s} > 1$ GeV/c. The second set exploited the long lifetime of the D^0 mesons, which have an average decay length $\langle L^0 \rangle \sim 1$ mm in $c\bar{c}$ events. We required: (2.i) x_{D^*} >0.2 ($K\pi$) or > 0.4 ($K\pi\pi\pi$); (2.ii) a probability $> 1\%$ for a vertex fit to the D^0 candidate tracks; and (2.iii) a D^0 decay length significance $L^0/\sigma_{L^0} > 2.5$.

Candidates for $D^+ \to K^-\pi^+\pi^+$ decays were formed by combining two same-sign pion candidate tracks with an opposite-sign kaon candidate. To reduce combinatoric background we required: (i) $x_{D^+} > 0.2$; (ii) all three tracks to have $p > 1$ GeV/c; (iii) $\cos\theta_K^+ > -0.8$, where θ_K^+ is the angle between the direction of the D^+ candidate in the laboratory frame and the K candidate in the D^+ rest frame; (iv) a vertex fit with $> 1\%$ probability; (v) a D^+ decay length significance $L^+/\sigma_{L^+} > 3.0$; (vi) the projection of the angle between the D^+ momentum vector and a line joining the IP and the vertex to be less than 20 mrad in the plane containing the track and the beam axis, and less than 15 (40) mrad in the x-y plane for $x_{D^+} < 0.4$ (> 0.4). To reject D^{*+} decays, the difference between the reconstructed $K\pi\pi$ invariant mass and each $K\pi$ invariant mass was required to be greater than 160 MeV/c^2.

4 Selection of Primary and Secondary D Mesons

In order to extract the number of D mesons in $c\bar{c}$ events, we defined 'c-rich' and 'b-rich' samples of candidates using information from the opposite hemisphere in the event, as well as the consistency of the D^0 or D^+ candidate with originating at the IP. We first applied an impact parameter technique [14] to hemispheres opposite to those containing a D meson candidate. In each such hemisphere we counted the number of "significant" tracks, N_{sig}^{opp}, having normalized transverse impact parameter with respect to the IP $\delta/\sigma_\delta > 3$. The distribution of this quantity is shown in fig. 1; the data are well described by our Monte Carlo simulation, and the simulation indicates that those candidates with high N_{sig}^{opp} are predominantly from $b\bar{b}$ events. The b-rich sample was defined by requiring $N_{sig}^{opp} \geq 3$.

Remaining D^{*+} candidates were accepted into the c-rich sample if they passed the cuts (2.i–2.iii) given above, the transverse impact parameter of the D^0 candidate momentum w.r.t. the IP, d_{xy}, was less than 20 μm, and the D^0 proper decay time,

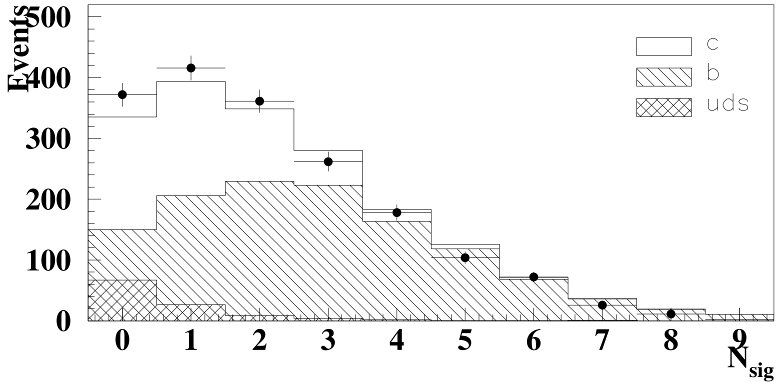

Figure 1: The distribution of the number of tracks in the hemisphere opposite a D meson candidate that miss the IP by at least 3σ. The points represent the data and the histogram represents the Monte Carlo simulation. The flavor composition of the simulation is indicated.

τ_{D^0}, was less than 1.0 ps. The distribution of the quantity d_{xy} is shown in fig. 2a for D^{*+} candidates that passed the cuts (2.i–2.iii) and had a mass difference (see below) in the range 142–149 MeV/c^2. The simulation describes the data well and shows that the primary charmed mesons typically have smaller impact parameters than the secondaries. Candidates that passed the cuts (1.i–1.iii) were also accepted into the c-rich sample. Remaining D^+ candidates were accepted into the c-rich sample if they satisfied $\phi_{xy} < 5$ (10) mrad for $x_{D^+} < 0.4$ (> 0.4). The distribution of the quantity ϕ_{xy} is shown in fig. 2b.

Distributions of the mass difference, $\Delta M = M_{D^0\pi_s} - M_{D^0}$, between the reconstructed invariant masses of the D^{*+} and D^0 candidates, are shown in fig. 3 for each of the $K\pi$ and $K\pi\pi\pi$ modes in the c-rich and b-rich samples. The results of a similar analysis of simulated data are also shown, indicating that the signal in the c-rich (b-rich) sample is predominantly from primary (secondary) D^{*+} mesons. The candidates in each sample were binned in scaled energy $x_{D^{*+}}$, and each ΔM distribution was fitted with a Gaussian signal function plus a background function of the form $A(\Delta M - M_\pi)^B$, where M_π is the charged pion mass and A and B are free parameters. The center and width of the signal function were fixed to values given by the simulation. The two decay modes of the D^0 were considered separately. The resulting estimates of the numbers of observed signal and combinatoric background candidates within ± 3.5 MeV/c of the

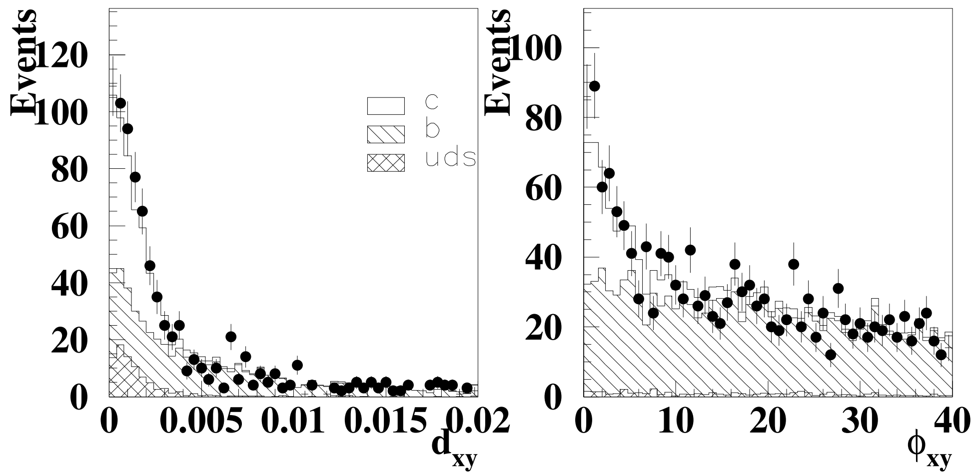

Figure 2: (a) The distribution of the transverse impact parameter of D^0 candidates in D^{*+} candidates with mass difference in the range 142–149 MeV/c^2. (b) Distribution of the angle between the momentum vector of a D^+ candidate with invariant mass in the range 1800–1940 MeV/c^2 and a line joining its measured decay vertex with the IP. The points represent the data and the histograms represent the Monte Carlo simulation, for which the flavor composition is indicated.

peak are listed in Table 1.

The invariant mass distributions of the $D^+ \to K^-\pi^+\pi^+$ candidates in the c-rich and b-rich samples are shown in figs. 3e and f, respectively. Again the simulation indicates good separation of primary from secondary mesons. The candidates in each sample were binned in x_{D+} and each mass distribution was fitted with a function comprising a Gaussian with fixed center and width for the D^+ signal and a third order polynomial function for the combinatoric background. The resulting estimates of the numbers of observed signal and combinatoric background candidates within ± 70 MeV/c of the peak are listed in Table 1.

For either the D^{*+} or D^+ mesons, the numbers of observed signal events in the c-rich and b-rich samples, N_{c-rich} and N_{b-rich} respectively, can be related to the numbers of D mesons produced in $c\bar{c}$ events ($N_{c\to D}$) and $b\bar{b}$ events ($N_{b\to D}$) as follows:

$$\begin{pmatrix} N_{c-rich} \\ N_{b-rich} \end{pmatrix} = \begin{pmatrix} \epsilon_c & \epsilon_b \\ \eta_c & \eta_b \end{pmatrix} \begin{pmatrix} N_{c\to D} \\ N_{b\to D} \end{pmatrix}. \qquad (1)$$

The tagging efficiencies, $\epsilon_{c,b}, \eta_{c,b}$, were estimated from the Monte Carlo simulation and

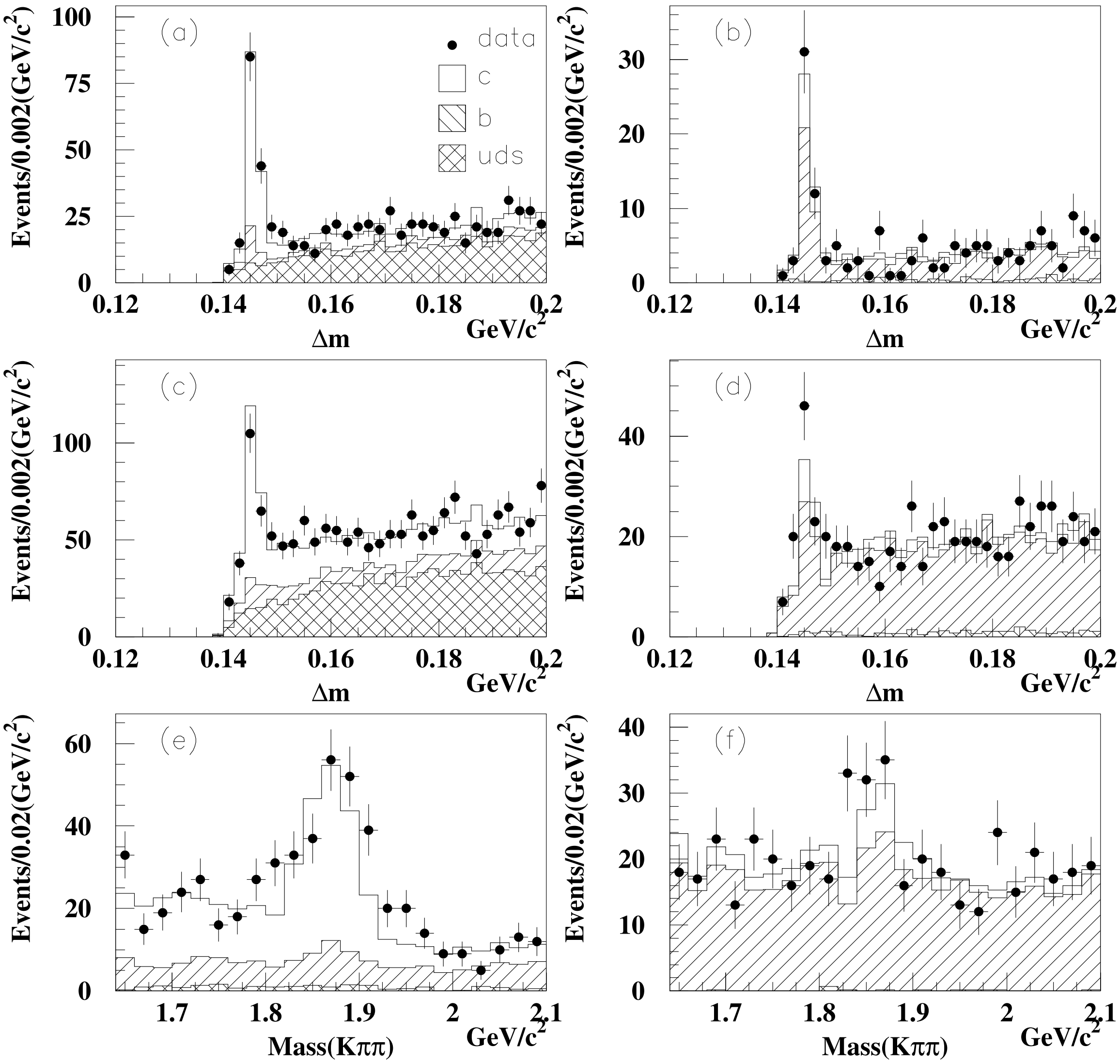

Figure 3: The ΔM distributions for $D^{*+} \to D^0 \pi_s^+$ candidates reconstructed in the (a,b) $D^0 \to K^- \pi^+$ and (c,d) $D^0 \to K^- \pi^+ \pi^- \pi^+$ modes and accepted into the (a,c) c-rich and (b,d) b-rich samples. The $M_{K\pi\pi}$ distribution for $D^+ \to K^- \pi^+ \pi^+$ candidates in the (e) c-rich and (f) b-rich samples. The points represent the data and the histograms represent the Monte Carlo simulation, for which the flavor composition is indicated.

x_D	$D^{*+} \to \pi_s^+(K^-\pi^+)$		$D^{*+} \to \pi_s^+(K^-\pi^+\pi^-\pi^+)$		$D^+ \to K^-\pi^+\pi^+$	
	c-rich	b-rich	c-rich	b-rich	c-rich	b-rich
0.2-0.4	15.6/10.4	36.4/43.6	–	–	25.6/52.4	27.8/169.2
0.4-0.5	34.9/23.1	27.5/ 7.5	9.5/23.5	22.3/ 38.7	40.1/38.9	8.9/ 99.1
0.5-0.6	23.2/ 8.8	10.3/ 3.7	32.6/71.4	18.7/ 15.3	38.3/28.7	21.0/ 33.0
0.6-0.7	21.9/ 4.1	4.2/ 1.8	27.9/26.1	6.6/ 2.4	29.3/13.7	6.5/ 12.5
0.7-1.0	21.2/ 2.8	4.8/ 0.2	17.8/ 9.2	10.9/ 1.1	43.6/13.4	21.3/ 2.7

Table 1: Observed numbers of signal/background events in the c-rich and b-rich samples for each D meson decay mode. The fitted background function was integrated over the regions $142 < \Delta M < 149$ MeV/c^2 and $1800 < M_{K\pi\pi} < 1940$ MeV/c^2.

are shown as functions of x_D in fig. 4. They include track and vertex reconstruction efficiencies that were checked using 3-prong τ-decays, which have a topology similar to that of D meson decays, in the simulation and the data. We solved eqn. 1 in each bin of x_D to obtain $N_{c\to D}$ and $N_{b\to D}$. The $N_{c\to D}$ were divided by the appropriate branching ratios, $BR(D^{*+} \to D^0\pi^+) = 68.1 \pm 1.6\%$ [15], $BR(D^0 \to K^-\pi^+) = 3.84 \pm 0.13\%$ [16], $BR(D^0 \to K^-\pi^+\pi^-\pi^+) = 7.5 \pm 0.4\%$ [16], and $BR(D^+ \to K^-\pi^+\pi^+) = 9.1 \pm 0.6\%$ [15], and divided by the number of accepted hadronic events to obtain total production rates of prompt charged D mesons per hadronic Z^0 decay. The corrected x_D distributions for prompt D^+ and D^{*+} mesons are shown in fig. 5.

5 Measurement of R_c

The fraction of hadronic Z^0 decays into $c\overline{c}$, R_c, may be written as:

$$R_c \equiv \frac{\Gamma_{c\overline{c}}}{\Gamma_{hadrons}} = \frac{N_{c\overline{d}} + N_{c\overline{u}} + N_{c\overline{s}} + \Sigma N_{cqq'}}{2N_{hadrons}}, \tag{2}$$

where $N_{c\overline{q}}$ represents the number of primary charm quarks that pair up with an antiquark of flavor q from the vacuum, $\Sigma N_{cqq'}$ represents the number that combine with any diquark pair to form a charmed baryon, and $N_{hadrons}$ is the total number of hadronic events. Assuming $N_{c\overline{u}} = N_{c\overline{d}}$, and defining a strangeness suppression parameter $S = N_{c\overline{s}}/N_{c\overline{d}}$ and a baryon suppression parameter $B = \Sigma N_{cqq'}/N_{c\overline{d}}$, one can

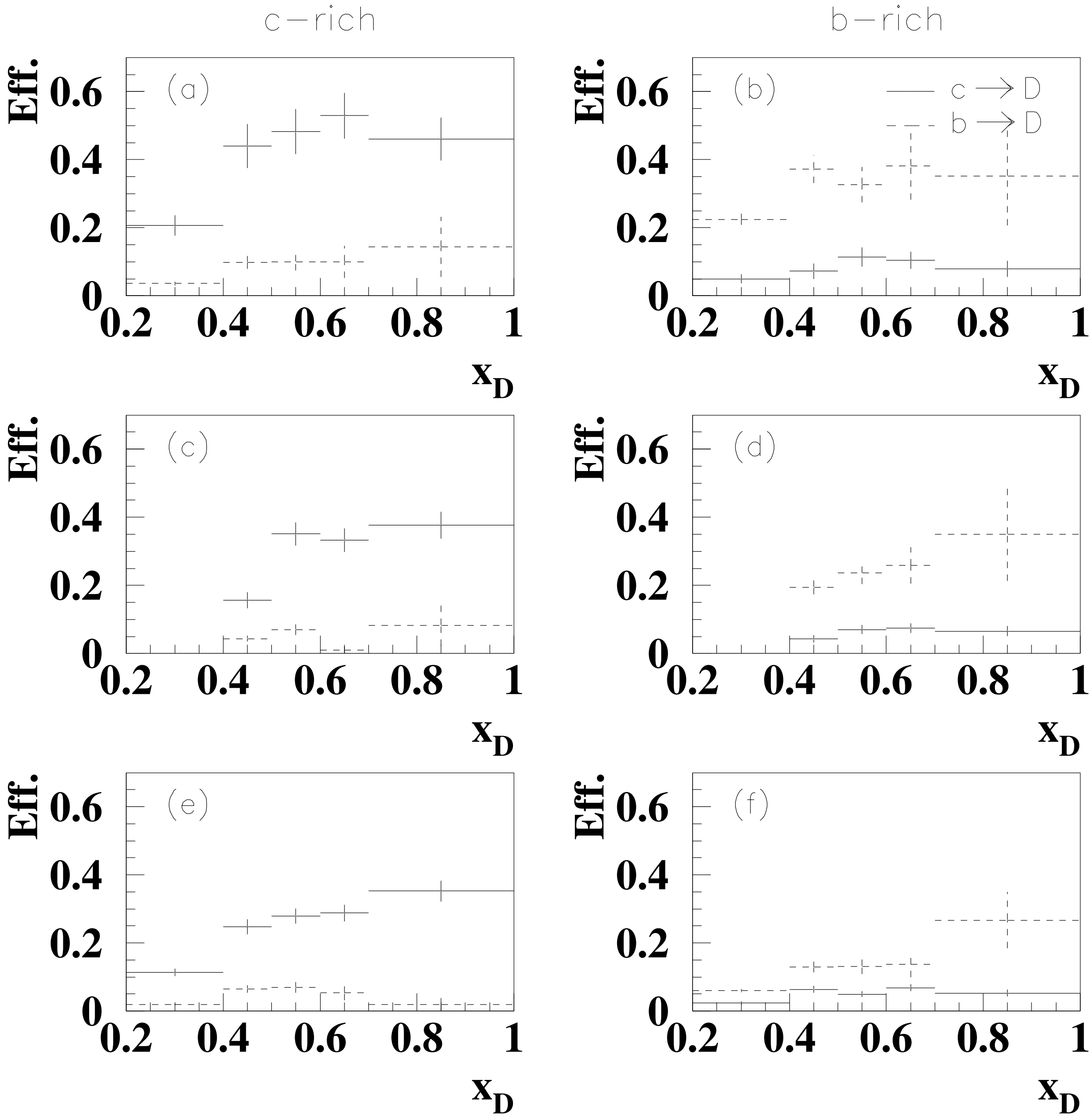

Figure 4: Simulated efficiencies for reconstructing true (a,b) $D^{*+} \to \pi_s^+ K^- \pi^+$, (c,d) $D^{*+} \to \pi_s^+ K^- \pi^+ \pi^+ \pi^+$, and (e,f) $D^+ \to K^- \pi^+ \pi^+$ decays and accepting them into the (a,c,e) c-rich or (b,d,f) b-rich sample. The solid (dashed) lines represent generated true primary (secondary) D-mesons.

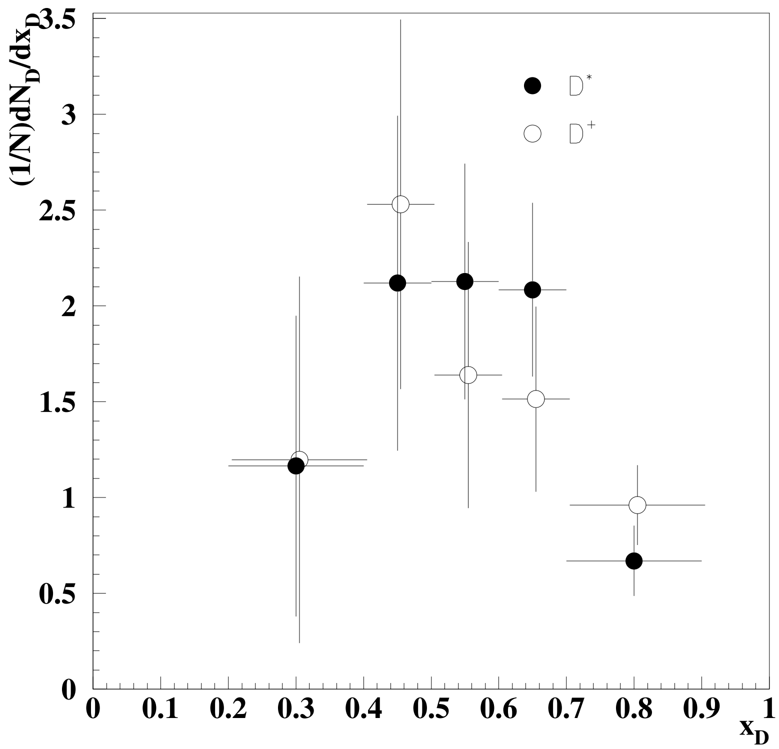

Figure 5: Distributions of scaled energy x_D for prompt charged vector (dots) and pseudoscalar (circles) charmed mesons. The errors are statistical and experimental systematic added in quadrature.

write

$$R_c = \frac{N_{c\bar{d}}(2+S+B)}{2N_{hadrons}}. \tag{3}$$

Under the assumptions that all primary $c\bar{d}$ pairs produce exactly one D^+ or D^{*+} meson and that there are no other sources of such mesons, the number of primary $c\bar{d}$ pairs can be equated to the total observed number of charged D^+ and D^{*+} mesons:

$$N_{c\bar{d}} = N_{c\to D^{*+}} + N_{c\to D^+}. \tag{4}$$

The second assumption is valid since neutral D^* mesons do not decay into charged D mesons, so that there are no contributions from primary $c\bar{u}$ or $c\bar{s}$ pairs, and D mesons from B hadron decays have been removed explicitly in our analysis. D mesons can be produced in hadronic events of any primary flavor q by gluon splitting, i.e. $Z^0 \to q\bar{q}g$, $g \to c\bar{c}$, but this is a small contribution to the total D meson rate, primarily at low x_D, and requires only a small correction to our measurement (see below). The production of excited D mesons, collectively referred to as D^{**}, in Z^0 decays has recently been reported [17]. However, their masses are well above those of the D and D^* mesons, so that isospin symmetry might be expected to hold. That is, we can assume that i) charged ($c\bar{d}$) and nonstrange neutral ($c\bar{u}$) D^{**} mesons are produced equally, and ii) all D^{**} mesons decay into a D or D^* meson, with $\mathrm{BR}(D^{**0} \to D^+X) = \mathrm{BR}(D^{**+} \to D^0X)$, etc. Under these assumptions, the equality (eqn. 4) holds exactly. We neglect the possible small effect of decays such as $D_s^{**} \to D^+X_s$ and $D^{**+} \to D_sX_{\bar{s}}$.

We integrated our measured D^+ and D^{*+} meson production rates over the range $0.2 < x_D < 1.0$. From these we subtracted gluon splitting contributions of roughly 1%, estimated from the simulation. We then applied correction factors of roughly 1.07 to account for the unmeasured region $x_D < 0.2$, which were also estimated from the simulation. We divided the sum of the corrected total numbers of D^+ and D^{*+} mesons by the number of accepted hadronic events to obtain $N_{c\bar{d}}/N_{hadrons} = 0.146 \pm 0.024$. We input this value into eqn. 3, along with values of the parameters S and B taken from measured relative rates of other strange mesons and baryons, $S = 0.3$ and $B = 0.2$, to obtain:

$$R_c = 0.182 \pm 0.027 \pm 0.012(\mathrm{Preliminary}), \tag{5}$$

where the first error is statistical and the second systematic. The components of the systematic error are discussed in section 8.

6 Measurement of P_V

The measured numbers of D^{*+} and D^+ mesons in $c\bar{c}$ events, $N_{c\to D^{*+}}$ and $N_{c\to D^+}$ respectively, can be related separately to $N_{c\bar{d}}$ via the relative vector to pseudoscalar meson production parameter $P_V = V/(P+V)$:

$$N_{c\bar{d}} \cdot P_V = N_{c\to D^{*+}}, \tag{6}$$

$$N_{c\bar{d}} \cdot (1 - P_V + (1 - BR_*)P_V) = N_{c\to D^+}, \tag{7}$$

where $BR_* = BR(D^{*+} \to D^0\pi^+)$ accounts for charged D^* mesons that do not decay to a charged pseudoscalar meson. Again, there are no contributions from primary $c\bar{u}$ or $c\bar{s}$ mesons, except for the effects of D^{**} decays, which we neglect here, though we note that the presence of such decays is not included in the theoretical predictions for P_V. Taking the ratio of the two equations, $N_{c\bar{d}}$ cancels, and we obtain:

$$\frac{N_{c\to D^{*+}}}{N_{c\to D^+}} = \frac{P_V}{1 - P_V BR_*} \ . \tag{8}$$

We considered the number of D^{*+} from each D^0 decay mode separately, and solved eqn. 8 in each bin of x_D. The resulting P_V values are listed in Table 2, and the average of the two modes is shown as a function of x_D in fig. 6. The errors are predominantly statistical. The systematic errors are discussed in section 8. Since the decay multiplicity of $D^{*+} \to \pi_s^+ K^- \pi^+$ is equal to that of $D^+ \to K^- \pi^+ \pi^+$ we are insensitive to uncertainties in track and vertex reconstruction efficiencies for this mode.

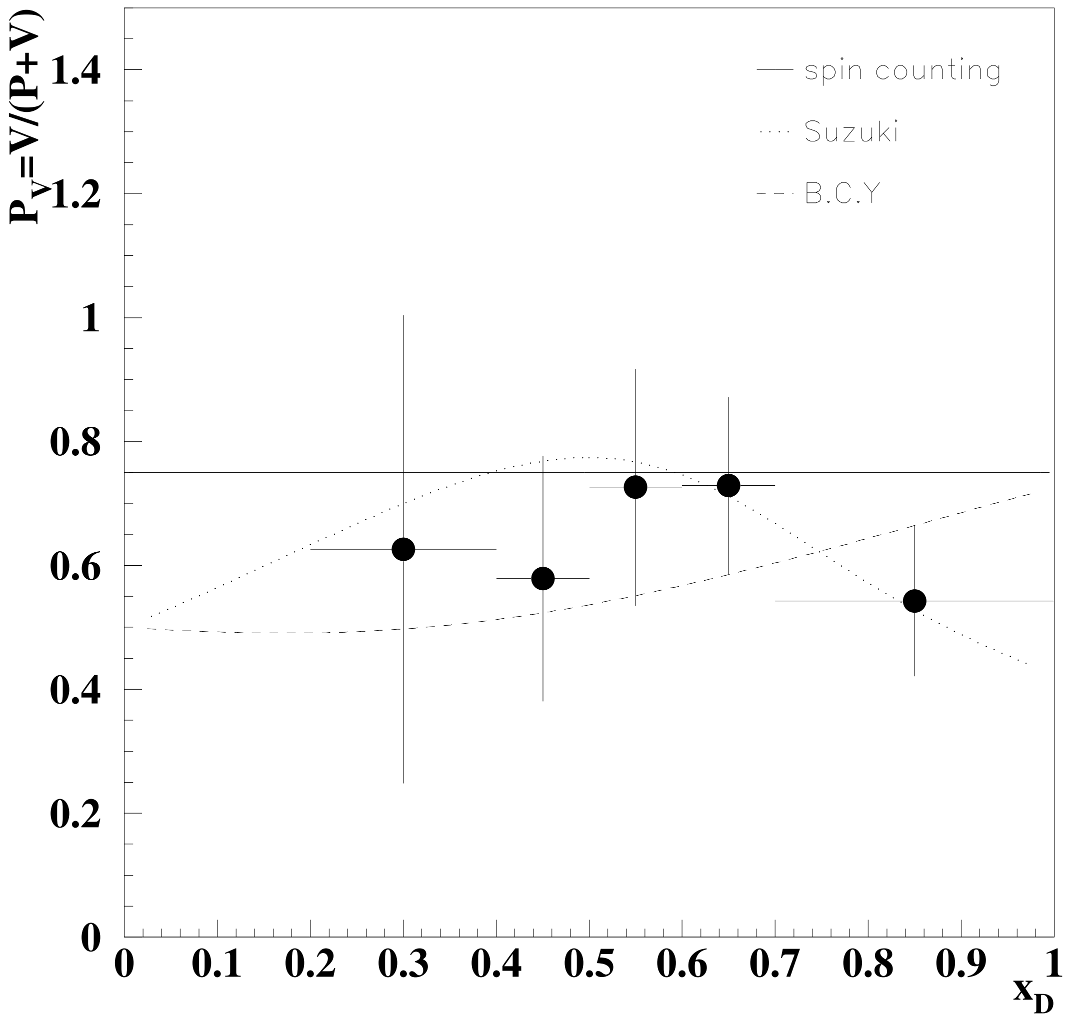

Figure 6: Preliminary measured P_V (dots) as a function of x_D. The solid line represents the expectation of naive spin counting, the dotted line is the calculation by Suzuki, and the dashed line is the calculation by Braaten et al.

The predictions of the QCD calculations of Braaten et al. and Suzuki are also shown in fig. 6, together with the prediction of naive spin counting, $P_V = 0.75$. All

x_D	$D^{*+} \to \pi_s^+(K^-\pi^+)$	$D^{*+} \to \pi_s^+(K^-\pi^+\pi^-\pi^+)$
0.2-0.4	0.63±0.38±0.03	–
0.4-0.5	0.71±0.19±0.03	0.28±0.39±0.02
0.5-0.6	0.73±0.20±0.03	0.72±0.23±0.04
0.6-0.7	0.72±0.16±0.03	0.75±0.16±0.04
0.7-0.9	0.69±0.14±0.03	0.45±0.14±0.03

Table 2: Preliminary P_V values as a function of x_D for the $K\pi$ and $K\pi\pi\pi$ modes. The first error is statistical and the second is experimental systematic.

predictions are consistent with the data. Averaging over the region $x_D > 0.4$, we obtain the preliminary result

$$P_V = 0.650 \pm 0.089(\text{stat.}) \pm 0.032(\text{syst.}) \pm 0.030(\text{BR}), \tag{9}$$

where the first error is statistical, the second one is systematic and the third is due to errors on relevant measured branching ratios. This result is consistent with both the spin counting hypothesis and previous measurements from the LEP experiments [1, 2], which yield an average of $P_V = 0.54 \pm 0.08$.

7 Measurement of D^{*+} Spin Alignment

We measured the degree of D^{*+} spin alignment along the flight direction by considering the angle θ^* between the momentum directions of the D^{*+} in the laboratory frame and the D^0 in the D^{*+} rest frame. For this measurement we used only those D^{*+} candidates passing the cuts (2.i–2.iii) given in section 4, since the cuts (1.i–1.iii) were found to bias the $\cos\theta^*$ distribution substantially. The analysis was performed on the inclusive sample passing these cuts, as well as on the corresponding c-rich and b-rich subsamples.

In each bin of x_{D^*} and $\cos\theta^*$ the $K\pi$ and $K\pi\pi\pi$ modes were combined and the number of candidates with mass difference in the window $142 < \Delta M < 149$ MeV/c^2 was counted. The number of expected combinatorial background candidates was subtracted, where the $\cos\theta^*$ dependence was taken from the simulation and the normalization was taken from a fit to the data in each x_{D^*} bin, integrated over $\cos\theta^*$. The results for the c-rich and b-rich samples were unfolded as described above, to yield $\cos\theta^*$ distributions for primary and secondary D^{*+} mesons. Normalized distributions of $\cos\theta^*$ for four x_{D^*}-bins are shown for the inclusive sample in fig. 7 before subtraction of the estimated background, which is also shown.

We then fitted the function:

$$\frac{1}{N}\frac{dN}{d\cos\theta^*} = \frac{3}{(6+2\alpha)}[1+\alpha\cos^2\theta^*], \tag{10}$$

to each distribution. The parameter α quantifies the degree of spin alignment and *a priori* can have any value in the range $-1 \leq \alpha \leq \infty$. For $\alpha = -1$, the decay-angular distribution is proportional to $\sin^2\theta$ and for $\alpha \to \infty$ the distribution is proportional to $\cos^2\theta$. The fitted values of α, α_c and α_b for inclusive, primary and secondary D^{*+} mesons, respectively, are listed in Table 3 for each x_{D^*} bin.

In fig. 8 we compare our inclusive results with similar measurements at lower c.m. energies from CLEO [18], HRS [19], and TPC [20]. All results are consistent with each other and with zero. In fig. 9 we compare our measured α_c for prompt D^* mesons with the predictions of Suzuki and Braaten et al. Our results disfavor the calculation of Suzuki. The prediction of spin counting, $\alpha_c = 0$, is also consistent with our data.

Averaging over the region $x_{D^*} > 0.4$, we obtain the preliminary results

$$\alpha = -0.072 \pm 0.300 \pm 0.357, \tag{11}$$

$$\alpha_c = 0.019 \pm 0.378 \pm 0.582, \tag{12}$$

$$\alpha_b = -0.484 \pm 0.549 \pm 0.219, \tag{13}$$

where the first error is statistical and the second is systematic. We summarize the systematic uncertainties in the next section. Our average value of α_c is consistent with that from a similar measurement, averaged over $x_{D^*} > 0.5$, from the OPAL experiment [21].

8 Systematic Errors

We have considered sources of systematic uncertainty that affect our various measurements of charmed hadron production. These can be divided into uncertainties in modelling the detector, uncertainties on experimental measurements serving as input

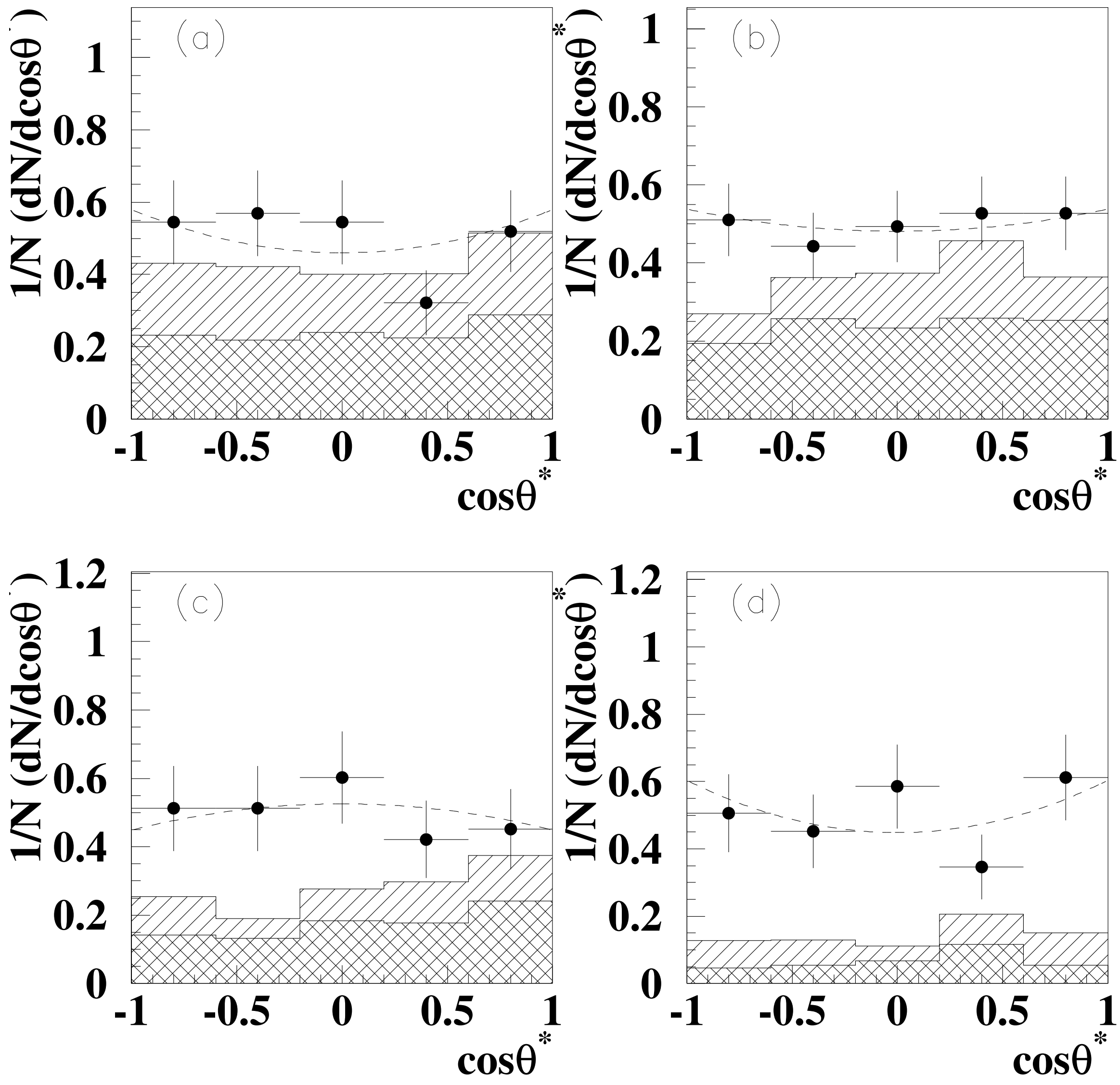

Figure 7: Distributions of $\cos\theta^*$ for the inclusive sample (dots) in four bins of x_{D^*}: (a) $0.2 < x_{D^*} < 0.4$, (b) $0.4 < x_{D^*} < 0.5$, (c) $0.5 < x_{D^*} < 0.6$, and (d) $0.6 < x_{D^*} < 1.0$. Also shown are the expected combinatoric background (cross-hatched histogram) and the expected contribution from B hadron decays (hatched histogram). The dashed lines represent the results of fits of eqn. 10, to which a constant has been added equal to the average background level.

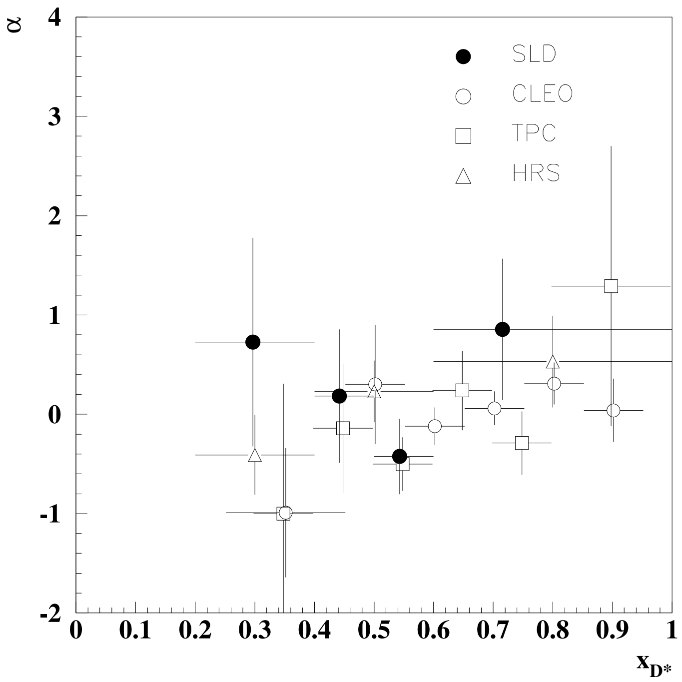

Figure 8: Preliminary fitted spin alignment parameter α (dots) for the inclusive sample of D^{*+} mesons from hadronic Z^0 decays, as a function of x_{D^*}. Also shown are similar results from experiments at lower c.m. energies.

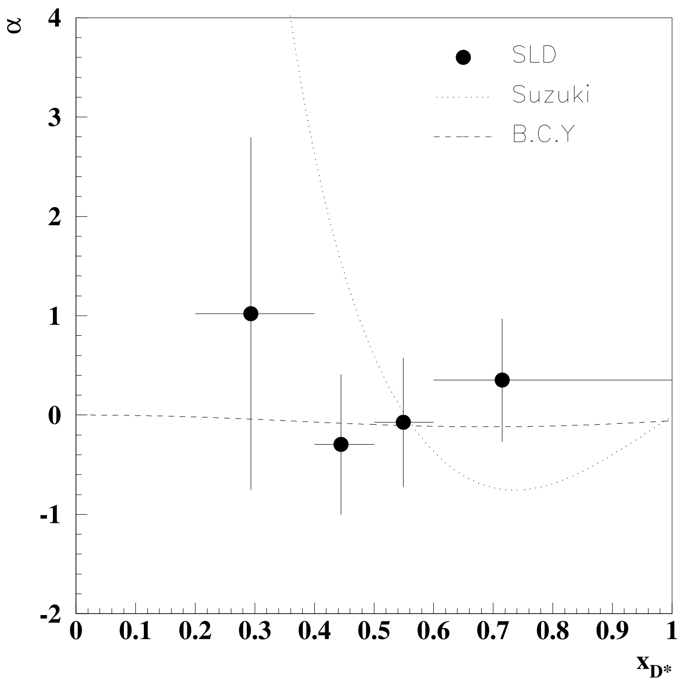

Figure 9: Preliminary fitted spin alignment parameter α_c for primary D^{*+} mesons as a function of x_{D^*}. The dotted line represents the calculation by Suzuki, and the dashed line the calculation by Braaten et al.

$\overline{x}_{D^*}$	α	α_c	α_b
0.30	0.73 ± 1.05	1.01 ± 1.77	0.59 ± 1.22
0.44	0.18 ± 0.67	-0.30 ± 0.70	0.59 ± 1.16
0.54	-0.42 ± 0.38	-0.07 ± 0.65	-0.90 ± 0.63
0.72	0.86 ± 0.71	0.35 ± 0.62	3.62 ± 4.04

Table 3: Preliminary spin alignment parameters α, α_c and α_b for inclusive, primary and secondary D^{*+}, respectively, as a function of x_{D^*}. Errors are statistical only.

parameters to the underlying physics modelling, and uncertainties in extracting signal rates from the measured invariant mass distributions. The various sources of systematic uncertainty are discussed in this section, and their effects on our x_D-averaged measurements are summarized in Table 4.

The dominant source of detector modelling uncertainty is the track reconstruction efficiency. This was measured using 3-prong τ decays in our data, a topology similar to our measured D meson modes, and the statistical error on that measurement was propagated as a systematic error for this analysis. This error cancels for P_V measured from the $K\pi$ mode, since a ratio of two 3-prong decay modes was used, and is small for the spin alignment measurements since it is independent of $\cos\theta^*$.

A large number of measured quantities relating to the production and decay of charm and bottom hadrons are used as input to our simulation, from which our reconstruction efficiencies are derived. Since we measured primary and secondary D meson production simultaneously, we are insensitive to the relative production of different D-meson species in B hadron decays, however we are sensitive to the properties of B hadron production and decay that affect the efficiencies for assigning candidates to the c-rich and b-rich samples, such as B hadron lifetimes and fragmentation functions. We considered systematic variations of input parameters given by world average measurements, derived in each case a new set of efficiencies $\epsilon_{c,b}, \eta_{c,b}$ from the simulation using an event weighting technique, and repeated the unfolding of the signals measured in the c- and b-rich samples. In the case of spin alignment, the background shape was also recalculated in each case. In addition, the R_c measurement is sensitive to the relative production of D_s mesons and charmed baryons.

Since there are small numbers of entries in many of the x_D bins used in the analysis, we are sensitive to the invariant mass range and the signal and background shapes used for fitting the data. Fits were performed using several alternative functional forms and various invariant mass ranges. We conservatively estimated a systematic error for the P_V and R_c measurements by taking the largest difference between results of any of these fits and the nominal values. For the spin alignment measurements, the $\cos\theta^*$-dependence of the background was checked using sideband data, and the full difference was assigned as a systematic error.

	P_V			Spin Alignment		
Error source	$K\pi$	$K\pi\pi\pi$	R_c	α_c	α_b	α
Tracking efficiency	–	1.0%	2.5%	–	–	–
B meson lifetime ($1.55 \pm 0.1ps$)	0.7%	0.9%	1.4%	0.005	0.012	0.008
B baryon lifetime ($1.1 \pm 0.3ps$)	0.1%	0.6%	0.9%	0.002	0.017	0.007
B baryon fraction (0.09 ± 0.03)	0.7%	1.2%	0.8%	0.004	0.006	0.006
Fragmentation	0.8%	1.6%	2.5%	0.013	0.038	0.022
$< x_b >= 0.700 \pm 0.011$						
$< x_c >= 0.494 \pm 0.012$						
Strangeness suppression ($\pm 10\%$)	–	–	1.2%	–	–	–
Charm Baryon fraction ($\pm 30\%$)	–	–	2.4%	–	–	–
Gluon splitting ($G = 0.03 \pm 0.015$)	–	–	0.7%	–	–	–
Fitting to extract signals	4.2%	12.5%	1.9%	0.582	0.215	0.356
Total Experimental	4.4%	12.8%	6.4%	0.582	0.220	0.357
D^0 , D^+ , D^{*+} Branching fractions	4.5%	5.6%	1.9%	–	–	–

Table 4: Summary of systematic uncertainties for the observables.

9 Summary and Conclusions

In conclusion, we have made preliminary measurements of the production of primary D^+ and D^{*+} mesons in hadronic Z^0 decays as a function of scaled energy. From the sum of the integrated numbers of these two particles we derived a measurement of

$$R_c = 0.182 \pm 0.027(\text{stat.}) \pm 0.012(\text{syst.}), \quad (\text{Preliminary}) \tag{14}$$

From the ratio of the two production rates we derived the relative vector to pseudoscalar production parameter $P_V = V/(V+P)$ for prompt charmed mesons as a function of x_D, and find the calculations of Suzuki and Braaten et al., as well as the prediction of the naive spin counting model, to be consistent with our measurement. Averaging over $x_D > 0.4$ we obtain

$$P_V = 0.650 \pm 0.089(\text{stat.}) \pm 0.032(\text{syst.}) \pm 0.030(\text{BR}), \quad (\text{Preliminary}) \tag{15}$$

consistent with previous measurements at the Z^0 resonance. We have measured the degree of spin alignment of inclusive, primary and secondary D^{*+} mesons along the flight direction as a function of x_{D^*}, finding all to be consistent with zero. The inclusive results are consistent with previous results at lower energies, and the measurements for primary D^* mesons are consistent with a recent result from OPAL. The calculation of Braaten et al. and the prediction of the naive spin counting model are consistent with the results for primary D^* mesons, and the calculation of Suzuki is disfavored.

Acknowledgments

We thank the personnel of the SLAC accelerator department and the technical staffs of our collaborating institutions for their outstanding efforts on our behalf.

*This work was supported by Department of Energy contracts: DE-FG02-91ER40676 (BU), DE-FG03-91ER40618 (UCSB), DE-FG03-92ER40689 (UCSC), DE-FG03-93ER40788 (CSU), DE-FG02-91ER40672 (Colorado), DE-FG02-91ER40677 (Illinois), DE-AC03-76SF00098 (LBL), DE-FG02-92ER40715 (Massachusetts), DE-FC02-94ER40818 (MIT), DE-FG03-96ER40969 (Oregon), DE-AC03-76SF00515 (SLAC), DE-FG05-91ER40627 (Tennessee), DE-FG02-95ER40896 (Wisconsin), DE-FG02-92ER40704 (Yale); National Science Foundation grants: PHY-91-13428 (UCSC), PHY-89-21320 (Columbia), PHY-92-04239 (Cincinnati), PHY-95-10439 (Rutgers), PHY-88-19316 (Vanderbilt), PHY-92-03212 (Washington); The UK Particle Physics and Astronomy Research Council

(Brunel and RAL); The Istituto Nazionale di Fisica Nucleare of Italy (Bologna, Ferrara, Frascati, Pisa, Padova, Perugia); The Japan-US Cooperative Research Project on High Energy Physics (Nagoya, Tohoku); The Korea Science and Engineering Foundation (Soongsil).

References

[1] ALEPH Collab., D. Buskulic *et al.*, Z.Phys **C62** (1994) 1.

[2] DELPHI Collab., P. Abreu *et al.*, Z.Phys **C59** (1993) 533.

[3] M. Suzuki, Phys. Rev. **D33** (1986) 676.

[4] E. Braaten *et al.*, Phys. Rev. **D51** (1995) 4819;
K. Cheung and T. C. Yuan, Phys. Rev. **D50** (1994) 3181.

[5] SLD Design Report, SLAC Report 273 (1984).

[6] M. D. Hildreth *et al.*, Nucl. Inst. Meth. **A367** (1995) 111.

[7] C. J. S. Damerell *et al.*, Nucl. Inst. Meth. **A288** (1990) 236.

[8] D. Axen *et al.*, Nucl. Inst. Meth. **A328** (1993) 472.

[9] A. C. Benvenuti *et al.*, Nucl. Inst. Meth. **A290** (1990) 353.

[10] S. Brandt *et al.*, Phys. Lett. **12** (1964) 57;
E. Farhi, Phys. Rev. Lett. **39** (1977) 1587.

[11] SLD Collab., K. Abe *et al.*, Phys. Rev. **D51** (1995) 962.

[12] T. Sjöstrand and M. Bengtsson, Comp. Phys. Comm. **43** (1987) 367.

[13] G. Marchesini *et al.*, Comp. Phys. Comm. **67** (1992) 465.

[14] SLD Collab., K. Abe *et al.*, Phys. Lett. **B386** (1996) 495.

[15] CLEO Collab., T. Butler *et al.*, Phys. Rev. Lett. **69** (1992) 2041.

[16] Particle Data Group, Phys. Rev. **D54** (1996) 1.

[17] ALEPH Collab., D. Buskulic *et al.*, Z. Phys. **C73** (1997) 601;
OPAL Collab. K. Ackerstaff *et al.*, CERN-PPE/97-035, submitted to Z. Phys. C.

[18] CLEO Collab., Y. Kubota *et al.*, Phys. Rev. **D44** (1991) 593.

[19] HRS Collab., S. Abachi *et al.*, Phys. Lett. **B199** (1987) 585.

[20] TPC Collab., H. Aihara *et al.*, Phys. Rev. **D43** (1991) 29.

[21] OPAL Collab. K. Ackerstaff *et al.*, Z. Phys. **C74** (1997) 437.

**List of Authors

K. Abe,(19) K. Abe,(30) T. Akagi,(28) N.J. Allen,(4) W.W. Ash,(28)† D. Aston,(28)
K.G. Baird,(24) C. Baltay,(34) H.R. Band,(33) M.B. Barakat,(34) G. Baranko,(9)
O. Bardon,(15) T. L. Barklow,(28) G.L. Bashindzhagyan,(18) A.O. Bazarko,(10)
R. Ben-David,(34) A.C. Benvenuti,(2) G.M. Bilei,(22) D. Bisello,(21) G. Blaylock,(16)
J.R. Bogart,(28) B. Bolen,(17) T. Bolton,(10) G.R. Bower,(28) J.E. Brau,(20)
M. Breidenbach,(28) W.M. Bugg,(29) D. Burke,(28) T.H. Burnett,(32) P.N. Burrows,(15)
W. Busza,(15) A. Calcaterra,(12) D.O. Caldwell,(5) D. Calloway,(28) B. Camanzi,(11)
M. Carpinelli,(23) R. Cassell,(28) R. Castaldi,(23)(a) A. Castro,(21) M. Cavalli-Sforza,(6)
A. Chou,(28) E. Church,(32) H.O. Cohn,(29) J.A. Coller,(3) V. Cook,(32) R. Cotton,(4)
R.F. Cowan,(15) D.G. Coyne,(6) G. Crawford,(28) A. D'Oliveira,(7) C.J.S. Damerell,(25)
M. Daoudi,(28) R. De Sangro,(12) R. Dell'Orso,(23) P.J. Dervan,(4) M. Dima,(8)
D.N. Dong,(15) P.Y.C. Du,(29) R. Dubois,(28) B.I. Eisenstein,(13) R. Elia,(28)
E. Etzion,(33) S. Fahey,(9) D. Falciai,(22) C. Fan,(9) J.P. Fernandez,(6) M.J. Fero,(15)
R. Frey,(20) T. Gillman,(25) G. Gladding,(13) S. Gonzalez,(15) E.L. Hart,(29)
J.L. Harton,(8) A. Hasan,(4) Y. Hasegawa,(30) K. Hasuko,(30) S. J. Hedges,(3)
S.S. Hertzbach,(16) M.D. Hildreth,(28) J. Huber,(20) M.E. Huffer,(28) E.W. Hughes,(28)
H. Hwang,(20) Y. Iwasaki,(30) D.J. Jackson,(25) P. Jacques,(24) J. A. Jaros,(28)
Z. Y. Jiang,(28) A.S. Johnson,(3) J.R. Johnson,(33) R.A. Johnson,(7) T. Junk,(28)
R. Kajikawa,(19) M. Kalelkar,(24) H. J. Kang,(26) I. Karliner,(13) H. Kawahara,(28)
H.W. Kendall,(15) Y. D. Kim,(26) M.E. King,(28) R. King,(28) R.R. Kofler,(16)
N.M. Krishna,(9) R.S. Kroeger,(17) J.F. Labs,(28) M. Langston,(20) A. Lath,(15)

J.A. Lauber,[9] D.W.G.S. Leith,[28] V. Lia,[15] M.X. Liu,[34] X. Liu,[6] M. Loreti,[21]
A. Lu,[5] H.L. Lynch,[28] J. Ma,[32] G. Mancinelli,[24] S. Manly,[34] G. Mantovani,[22]
T.W. Markiewicz,[28] T. Maruyama,[28] H. Masuda,[28] E. Mazzucato,[11]
A.K. McKemey,[4] B.T. Meadows,[7] R. Messner,[28] P.M. Mockett,[32]
K.C. Moffeit,[28] T.B. Moore,[34] D. Muller,[28] T. Nagamine,[28] S. Narita,[30]
U. Nauenberg,[9] H. Neal,[28] M. Nussbaum,[7]† Y. Ohnishi,[19] N. Oishi,[19]
D. Onoprienko,[29] L.S. Osborne,[15] R.S. Panvini,[31] C.H. Park,[27] H. Park,[20]
T.J. Pavel,[28] I. Peruzzi,[12][b] M. Piccolo,[12] L. Piemontese,[11] E. Pieroni,[23]
K.T. Pitts,[20] R.J. Plano,[24] R. Prepost,[33] C.Y. Prescott,[28] G.D. Punkar,[28]
J. Quigley,[15] B.N. Ratcliff,[28] T.W. Reeves,[31] J. Reidy,[17] P.L. Reinertsen,[6]
P.E. Rensing,[28] L.S. Rochester,[28] P.C. Rowson,[10] J.J. Russell,[28] O.H. Saxton,[28]
T. Schalk,[6] R.H. Schindler,[28] B.A. Schumm,[6] J. Schwiening,[28] S. Sen,[34]
V.V. Serbo,[33] M.H. Shaevitz,[10] J.T. Shank,[3] G. Shapiro,[14] D.J. Sherden,[28]
K.D. Shmakov,[29] C. Simopoulos,[28] N.B. Sinev,[20] S.R. Smith,[28] M.B. Smy,[8]
J.A. Snyder,[34] H. Staengle,[8] P. Stamer,[24] H. Steiner,[14] R. Steiner,[1]
M.G. Strauss,[16] D. Su,[28] F. Suekane,[30] A. Sugiyama,[19] S. Suzuki,[19]
M. Swartz,[28] A. Szumilo,[32] T. Takahashi,[28] F.E. Taylor,[15] E. Torrence,[15]
A.I. Trandafir,[16] J.D. Turk,[34] T. Usher,[28] J. Va'vra,[28] C. Vannini,[23] E. Vella,[28]
J.P. Venuti,[31] R. Verdier,[15] P.G. Verdini,[23] D.L. Wagner,[9] S.R. Wagner,[28]
A.P. Waite,[28] S.J. Watts,[4] A.W. Weidemann,[29] E.R. Weiss,[32] J.S. Whitaker,[3]
S.L. White,[29] F.J. Wickens,[25] D.C. Williams,[15] S.H. Williams,[28] S. Willocq,[28]
R.J. Wilson,[8] W.J. Wisniewski,[28] M. Woods,[28] G.B. Word,[24] J. Wyss,[21]
R.K. Yamamoto,[15] J.M. Yamartino,[15] X. Yang,[20] J. Yashima,[30] S.J. Yellin,[5]
C.C. Young,[28] H. Yuta,[30] G. Zapalac,[33] R.W. Zdarko,[28] and J. Zhou,[20]

[1] *Adelphi University, Garden City, New York 11530*
[2] *INFN Sezione di Bologna, I-40126 Bologna, Italy*
[3] *Boston University, Boston, Massachusetts 02215*
[4] *Brunel University, Uxbridge, Middlesex UB8 3PH, United Kingdom*
[5] *University of California at Santa Barbara, Santa Barbara, California 93106*
[6] *University of California at Santa Cruz, Santa Cruz, California 95064*
[7] *University of Cincinnati, Cincinnati, Ohio 45221*
[8] *Colorado State University, Fort Collins, Colorado 80523*
[9] *University of Colorado, Boulder, Colorado 80309*

[10] Columbia University, New York, New York 10027
[11] INFN Sezione di Ferrara and Università di Ferrara, I-44100 Ferrara, Italy
[12] INFN Lab. Nazionali di Frascati, I-00044 Frascati, Italy
[13] University of Illinois, Urbana, Illinois 61801
[14] E.O. Lawrence Berkeley Laboratory, University of California, Berkeley, California 94720
[15] Massachusetts Institute of Technology, Cambridge, Massachusetts 02139
[16] University of Massachusetts, Amherst, Massachusetts 01003
[17] University of Mississippi, University, Mississippi 38677
[18] Moscow State University, Institute of Nuclear Physics 119899 Moscow, Russia
[19] Nagoya University, Chikusa-ku, Nagoya 464 Japan
[20] University of Oregon, Eugene, Oregon 97403
[21] INFN Sezione di Padova and Università di Padova, I-35100 Padova, Italy
[22] INFN Sezione di Perugia and Università di Perugia, I-06100 Perugia, Italy
[23] INFN Sezione di Pisa and Università di Pisa, I-56100 Pisa, Italy
[24] Rutgers University, Piscataway, New Jersey 08855
[25] Rutherford Appleton Laboratory, Chilton, Didcot, Oxon OX11 0QX United Kingdom
[26] Sogang University, Seoul, Korea
[27] Soongsil University, Seoul, Korea 156-743
[28] Stanford Linear Accelerator Center, Stanford University, Stanford, California 94309
[29] University of Tennessee, Knoxville, Tennessee 37996
[30] Tohoku University, Sendai 980 Japan
[31] Vanderbilt University, Nashville, Tennessee 37235
[32] University of Washington, Seattle, Washington 98195
[33] University of Wisconsin, Madison, Wisconsin 53706
[34] Yale University, New Haven, Connecticut 06511
† Deceased
[a] Also at the Università di Genova
[b] Also at the Università di Perugia